

Laser induced changes in the optical properties of PVA/PEG blend loaded with graphene oxides

Emad Mousa

Physics Department, Faculty of Science
Cairo University, Egypt
emad@sci.cu.edu.eg

Magdy M Omar

Physics Department, Faculty of Science
Cairo University, Egypt
magdymomar@gmail.com

Mohamed Fikry

Physics Department, Faculty of Science
Cairo University, Egypt
mfikry@sci.cu.edu.eg

Dalia Refaat

Basic science Department, Faculty of Engineering
Egyptian Russian University, Egypt
daliarefaat91@gmail

Abstract— Plasticized PVA/PEG (80/20 wt%) blends loaded with different concentrations of graphene oxide (0, 0.5, 1.5, 3 wt%) were prepared by simple solution casting method. Samples were exposed to continuous Argon laser beam of power 30 mW for different periods of (30, 45, 60 min.). The optical properties of prepared samples were studied before and after laser irradiation to investigate the effect of both graphene oxide loading and laser exposure time. The absorption spectra were analyzed to calculate the energy band gap and band tail width. Besides, dispersion of refractive index has been analyzed using the Wemple–DiDomenico single oscillator model. Dispersion parameters, optical dielectric constant, plasma frequency have been calculated for the investigated samples.

Keywords—PVA; PEG; GO; OPTICAL PROPERTIES ; Laser irradiation

I. INTRODUCTION

Polyvinyl Alcohol (PVA) is one of polymeric materials that have wide range of applications. This is mainly due to their good optical properties, lightweight, good mechanical properties. PVA has many uses such as adhesives, coatings, drug delivery systems and fuel cells [1]. Owing to the strong inter and intramolecular hydrogen bonds between hydroxyl groups, PVA has a high melting point that is close to its decomposition temperature which makes its melt processing very difficult and hence, PVA has been processed mainly from aqueous solutions.

Polyethylene glycol (PEG) is a water-soluble synthetic polymer widely used in pharmaceutical and cosmetic industry. PEG has many properties such as wide range of molecular weight, low toxicity, and chain flexibility, and it has been used frequently in the production of polymer blends as it can improve the flexibility and ductility of rigid polymers [2].

In the present study, PVA and PEG were chosen as the host polymers because both polymers are water soluble and can also form a variety of hydrogen bonding interactions with various fillers. Also, both

Polymers are highly compatible with each other and form miscible blends through hydrogen bonding interactions between the hydroxyl groups of PVA and the ether linkage of PEG chains [3].

Graphene Oxide (GO) has several applications such as supercapacitors, memory devices, optoelectronics, photocatalysis, drug delivery, and composite materials [4], [5]. The intriguing properties of GO have drawn the attention of the scientific community very recently. Therefore, it would be interesting to develop eco-friendly polymer/GO composite material suitable for commodity and technological applications.

A lot of research work [6]–[8] devoted to study the effect of laser irradiation, annealing, γ - irradiation and so forth on optical and physical properties of polymeric materials. In the radiation processing of materials by laser, several changes occur in optical properties of composites. So, it is important to study the effect of laser treatment on the optical properties of our pure and graphene oxide loaded PVA/PEG blends.

In short, the aim of this work is to study the effect of GO loadings on the optical properties of (80/20) PVA/PEG blend, alongside the effect of laser irradiation duration time on the optical properties of prepared samples.

II. EXPERIMENTAL

A. Materials :

PVA ($M_w=72000$ g.mol⁻¹, degree of hydrolysis 97.5-99.5 mol%) and PEG ($M_w=5000-7000$ g.mol⁻¹) were purchased from Fluka, Germany. Graphite fine powder (<50 μ m) was Purchased from Merk, Germany. H₂SO₄ (98%), H₃PO₄ (85%), HCL, and Hydrazine hydrate were purchased from Sigma-Aldrich, USA. Glycerine (Ash \leq 0.02%), KMNO₄, H₂O₂ (35%), and Ethanol (96%) were supplied by El Nasr Pharmaceutical chemicals Company, Egypt.

B. Preparation:

Graphene oxide (GO) was prepared from graphite based on improved Hummer's method as reported elsewhere [9].

PVA/PEG blends were prepared by solution casting technique. The PVA powder was dissolved in deionized water at 90 °C for 1hr with continuous stirring until complete miscibility. Meanwhile, PEG was dissolved in deionized water at room temperature. Both solutions were mixed and stirred for additional 1 hr, and then 1 gm of glycerine was added to the mixture with continuous stirring for an additional 1hr.

To prepare graphene oxide loaded samples, GO was dispersed in 10 ml deionized water using ultrasonicator for 20 min. before being added with different concentrations to the PVA/PEG (80/20 wt%) blend. Glycerol plasticized PVA/PEG blend was loaded with different concentrations of graphene oxide (0, 0.5, 1.5, 3 wt%).

Finally, mixed solutions were poured onto glass Petri dishes and left to dry at room temperature for 48 hrs.

C. Techniques:

Laser irradiation of samples was applied by continuous Argon laser beam of power 30 mWatt for different periods of (30, 45, 60 min.).

Optical measurements for irradiated and unirradiated samples were carried out using a Shimadzu UV 3600 plus UV-VIS-NIR spectrophotometer in the range 200-2500 nm in step of 5 nm.

III. RESULTS AND DISCUSSION

1) Optical properties of GO loaded PVA/PEG Blend:

One of the most productive methods in developing and understanding the structure and energy gap of amorphous non-metallic materials is the study of their optical absorption spectra.

Figure (1) represents the absorption spectra of different GO loaded samples before exposure to laser beam. Figure (1) reveals that the intensity of absorption increases by increasing the graphene oxide concentration up to 1.5 wt % and then followed by slight decrease with further loading up to 3 wt%. Moreover, one can estimate the absorption coefficient $a(\lambda)$ for all composites from the following equation (1):

$$a(\lambda) = \frac{2.3 \log \left(\frac{I_i}{I_t} \right)}{t} = 2.3 \left(\frac{A}{t} \right) \quad (1)$$

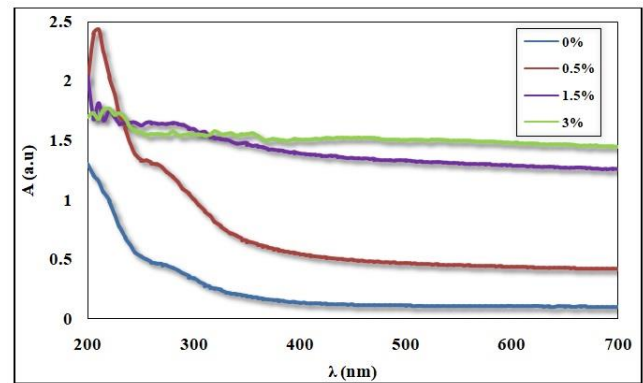


Fig. 1. Absorption spectra of different concentrations of GO loaded PVA/PEG composites.

Where I_i and I_t are the intensity of the incident and transmitted light, respectively. A is the absorbance and t is the sample thickness. The observed increase in absorption coefficient with graphene oxide loading (as shown in Figure (2)) may be due to the existence of more transitions from higher vibration levels of the ground state to higher sublevels of the first excited singlet state [10].

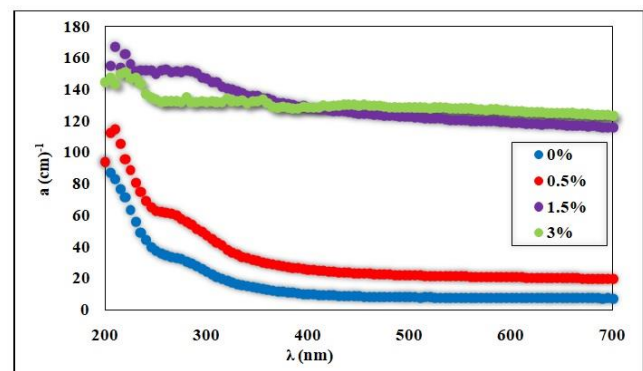


Fig. 2. Absorption coefficient of all samples.

A. Interband transitions:

Davis and Mott [11] formulate an equation to express the dependence of the absorption coefficient, a , on the photon energy $E=h\nu$ of the quantum radiation absorbed by the material as given by equation (2):

$$aE = C(E - E_g)^n \quad (2)$$

where C is a constant called the band tailing parameter, E_g is the optical band gap of the sample, and n is the power index having the values of 2, 3, 1/2 and 3/2 referring to the nature of electronic transition responsible for the absorption [12].

A straight line in the UV region is observed for the plot of $(aE)^{1/2}$ versus the photon energy E for all samples as presented in Figure (3), and E_g values were deduced from the intercept with x-axis. The electronic transitions are indirect allowed transitions as detected for many non-crystalline materials, and E_g values are tabulated in Table (1).

Table (1): The indirect optical energy gap and Urbach energy of all tested samples.

GO wt %	E_g (eV)	E_u (eV)
0	3.5	1.06
0.5	3.2	2.05
1.5	3	8.8
3	2.6	8.7

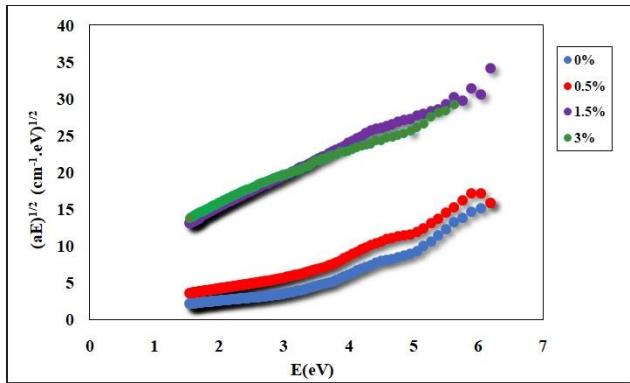


Fig. 3. Variation of $(\alpha E)^{1/2}$ with the photon energy E for all tested samples.

B. Urbach energy:

An extending tail for lower photon energies was clarified in the absorption spectra below the band edge, which can be described by [13]:

$$a = a_0 \exp\left(\frac{E}{E_u}\right) \quad (3)$$

where E_u is the energy of Urbach corresponding to the width of the band tail of localized states in the band gap. From the reciprocal gradient of the linear portion of the plot of $\ln(a)$ versus E presented in Figure (4), E_u values were calculated and tabulated in Table (1). It is observed that the values of the band tail width E_u was decreased from 1.6 to 8.8 eV with the addition of GO.

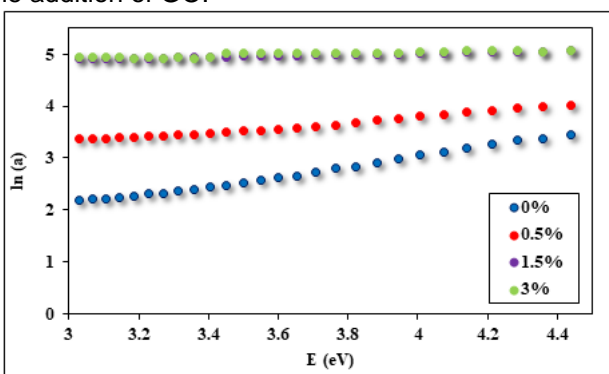


Fig. 4. Dependence of $\ln(a)$ upon the photon energy E for all samples.

C. Optical constants:

The attenuation coefficient (η) [14] of the medium is directly proportional to the absorption coefficient (a) according to the equation:

$$a = \frac{4\pi\eta}{\lambda} \quad (4)$$

Where λ is the free space wavelength of light.

The reflection coefficient (ρ), for normal incidence, is given by [15]:

$$\rho = \frac{(m-1)^2 + \eta^2}{(m+1)^2 + \eta^2} \quad (5)$$

Applying equations (4) & (5) with the aid of absorption and reflection spectra, one can calculate the optical constants (refractive index m and the attenuation coefficient η).

Figure (5) shows the wavelength, λ , dependence of the refractive index for pure PVA/PEG blend and GO loaded composites.

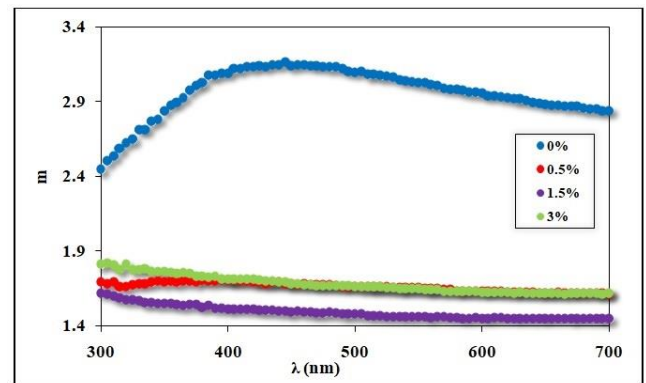


Fig. 5. Variation of refractive index (m) as a function of wavelength (λ) for all samples.

It is noticed from this figure that the refractive index values of GO loaded PVA/PEG nanocomposites are lower than the refractive index of virgin PVA/PEG and it decreases with further GO loading. The addition of GO nanoparticles in PVA/PEG matrix may be responsible for the formation of localized electronic states in the highest occupied molecular orbital-lowest unoccupied molecular orbital (HOMO-LUMO) gap [16], [17].

These localized electronic states govern the optical and electrical properties of the host material. Their role as trapping centers (here), depress the low energy transitions, leading to the observed change in refractive index.

It is also clear from Figure (5) that for loaded PVA/PEG, refractive index decreases with increasing wavelength showing normal dispersion. But in case of PVA/PEG virgin sample, refractive index decreases in the wavelength range 465-700 (nm) displaying normal dispersion, and exhibiting an anomalous behavior as it increases with increasing wavelength from 300-500 nm.

D. Dispersion energy:

The dispersion energy has an important role in the field of optical properties owing to its significance in optical communication and designing devices. Wemple and DiDomenico [18] used a simple single oscillator model to analyze the refractive index normal dispersion. According to their analysis, the refractive index m at frequency (ν) in terms of both dispersion

energy E_d (which is a measure of the strength of optical transition) and single oscillator energy E_s can be written as [19]:

$$m^2 - 1 = \frac{E_d E_s}{(E_s^2 - E^2)} \quad (6)$$

From the intercept and slope of the linear fitted lines of $(m^2 - 1)^{-1}$ against E^2 , as shown in Figure (6), the values of E_d and E_s obtained and tabulated in Table (2).

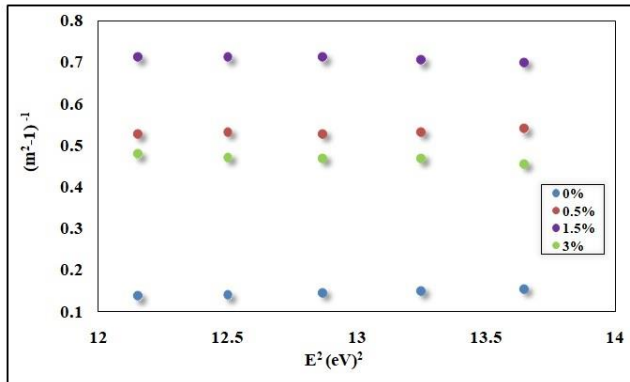


Fig. 6. Dependence of $(m^2 - 1)^{-1}$ on E^2 for GO loaded PVA/PEG samples.

It is observed from Table (2) that both values of E_d and E_s decrease with increasing concentration of GO particles in PVA/PEG matrix. So, the dispersion of the refractive index is inversely related to both E_d and E_s as confirmed by DiDomenico and Wemple [18]. The decreasing behavior of both E_d and E_s with GO loading may be due to the increasing behavior in localized electronic state which in turn enhances the low energy transitions.

Table (2): Values of optical parameters with respect to GO content in PVA/PEG blend.

GO wt%	E_d (eV)	E_s (eV)
0	31.6	12.6
0.5	14.6	8.1
1.5	9.3	6.9
3	6.3	3.2

E. Optical Dielectric Constant:

Both the real and imaginary parts of the dielectric constant are related to the refractive index (n) and extinction (attenuation) coefficient (η) values as [20], [21]:

$$\epsilon' = m^2 - \eta^2 = \epsilon_\infty - \frac{e^2 N}{\pi C^2 m^*} \lambda^2 \quad (7)$$

$$\epsilon'' = 2m\eta = \frac{\epsilon_\infty w_p^2}{8\pi C^3 \tau} \lambda^3 \quad (8)$$

where w_p is the plasma resonance frequency for one kind of free carriers and is given by:

$$w_p = \left(\frac{e^2 N}{\epsilon_0 \epsilon_\infty m^*} \right)^{\frac{1}{2}} \quad (9)$$

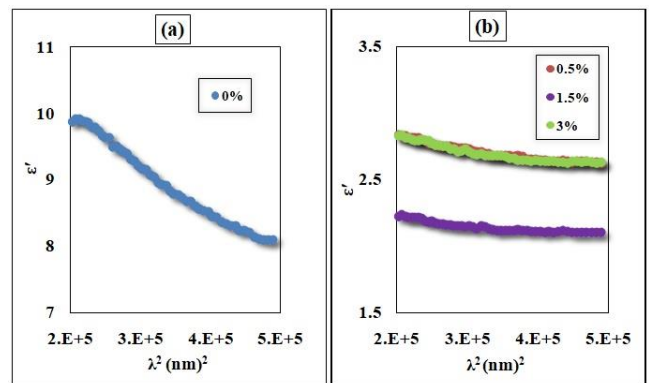


Fig. 7. Dependence of the real part of the dielectric function ϵ' on λ^2 .

where ϵ_0 is the free space dielectric constant, e is the electronic charge, ϵ_∞ is the residual dielectric constant, N/m^* is the ratio of free carrier concentration N to the effective mass m^* , c is the light velocity, and τ is the optical relaxation time.

Both the values of (N/m^*) and ϵ_∞ could be obtained by plotting graph between ϵ' and λ^2 which is found to be straight line as shown in Figure (7) and tabulated in Table (3). By using equation (9), the plasma resonance frequency (w_p) for free carriers was calculated. Taking into account that m^* is constant, so the increasing behavior of w_p with GO loading may be ascribed to the increase of carrier concentration N as tabulated in Table (3).

Table (3): Values of optical parameter with respect to GO content in PVA/PEG matrix.

GO wt%	ϵ_∞	$N/m^* (10^{48})$	$W_p (10^{11} \text{ Hz})$
0	10	77	3
0.5	2.8	10	1.01
1.5	2.6	12	1.15
3	2.8	14	1.2

2) Laser Induced Changes of the optical properties:

A. Absorption spectra:

Owing to its good optical properties relative to other GO loaded samples, the effect of laser radiation exposure time on the 0.5% GO loaded sample will be compared to that of pure sample. The absorption spectra of 0% and 0.5% GO loaded PVA/PEG samples are illustrated in Figure (8) at different laser exposure time.

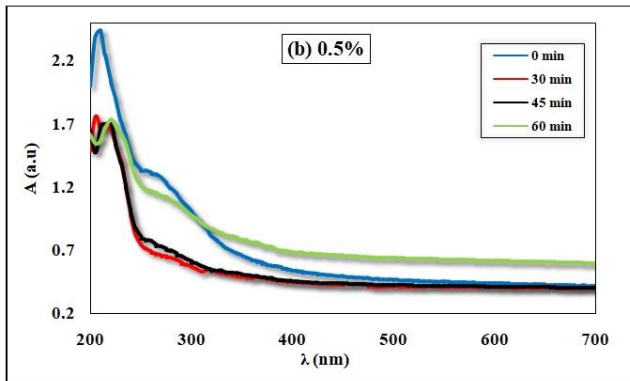
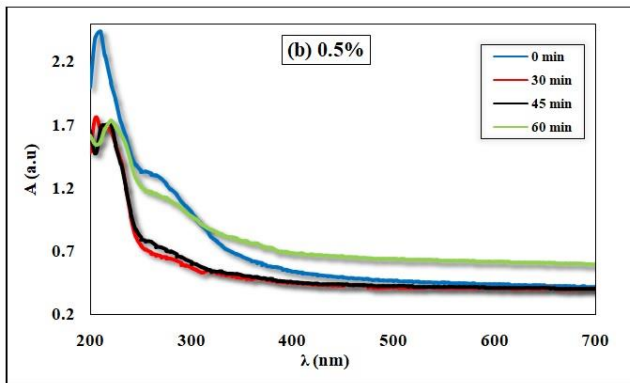


Fig. 8. Absorption spectra after laser irradiation for a. 0% b. 0.5% GO loaded PVA/PEG blend.

One could observe a decrease in the absorbance spectra of all samples with the increase of the applied laser energies up to 900 mJ (30 min.) and increases with greater energy dose. Moreover, there was a shift in the absorption edge towards higher energies (shorter wavelength) with laser energies for virgin sample in accordance to Moss-Burstein effect [22]. Meanwhile, a reverse behavior was observed to plasticized blend loaded with 0.5 wt% of GO filler. This behavior could be owed to the increasing optical absorption and increasing attenuation of incident beam [23].

Figure (9) show the dependence of the absorption coefficient on the wavelength for 0% and 0.5% GO loaded PVA/PEG samples, respectively, before and after being irradiated with laser for (30, 45 and 60 min.) exposure time.

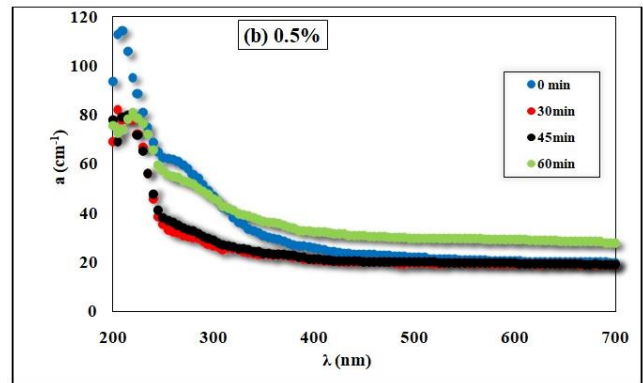


Fig. 9. The variation of the absorption coefficient as a function of wavelength before and after laser irradiation for a. 0% and b. 0.5% GO loaded PVA/PEG composites.

Meanwhile, Figure (10) is employed to determine the change in the energy gap E_g due to the laser irradiation energies.

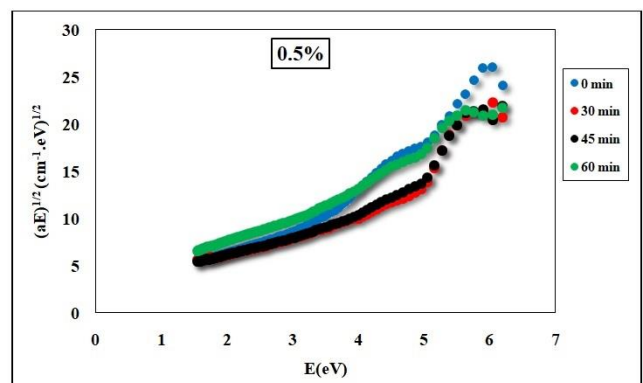
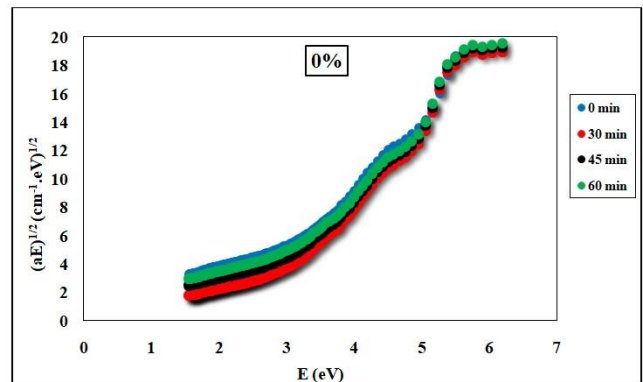
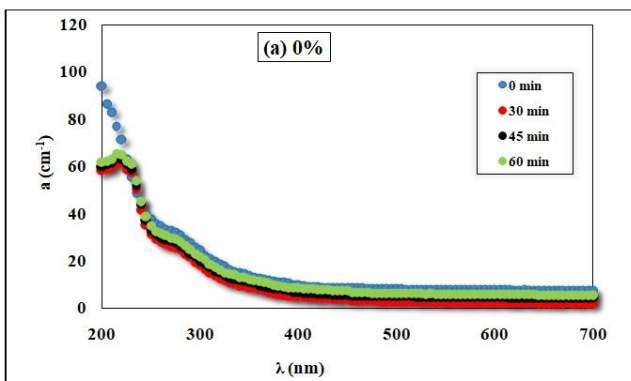


Fig. 10. Variation of $(aE)^{1/2}$ with the photon energy E for a. 0% and b. 0.5% GO loaded PVA/PEG composites.

It can be seen that, a, decreases with the increase of laser energies up to 900 mJ (30 min.) and begins to increase with further energies greater than 900 mJ. During laser irradiation up to 900 mJ, the sample gets enough vibration energy that converted to bulk heating and the defects are gradually reduced. Meanwhile, beyond 900 mJ laser energy, the samples were over heated and new defects appear which explains the increasing behavior of absorption coefficient. The reduction of defects decreases the density of localized states (Urbach energy E_u) in the band structure, and consequently increasing the



optical gap (E_g) up to 1800 mJ (60 min.) of laser beam, as shown in Table (4).

Table (4): Represents the radiation dose dependence of the energy gap of plasticized blend and GO loaded one.

Doses time (min.)	E_g (eV)	
	0% GO	0.5% GO
0	3.5	3.2
30	3.6	3.5
45	3.7	3.7
60	3.8	3.2

B. Optical Constants:

Equations (4), (5), and (6) were used, respectively, to calculate the attenuation and reflection coefficients and refractive index of the irradiated samples.

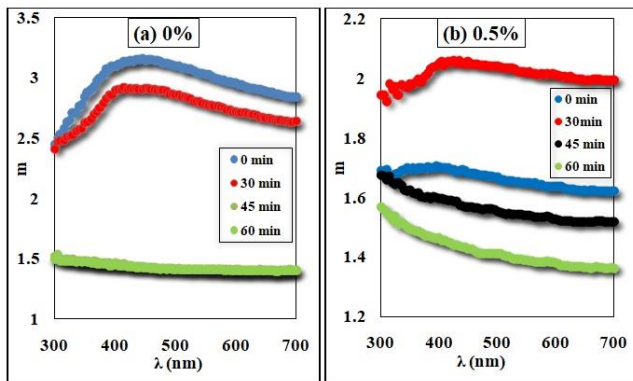


Fig. 11. Variation of refractive index with the wavelength for a. 0% and b. 0.5% GO loaded PVA/PEG composites.

It is noticed from Figure (11) that the refractive index of both tested samples decreases appreciably by increasing laser energy up to 1350 mJ (45 min.). The refractive index decreases by 33 % upon laser exposure (≤ 60 min.) for pure sample and firstly increases by 17% for 0.5% GO loaded sample at laser radiation dose of (30 min.) and then after decreases by 20% upon further laser irradiation dose greater than 30 min. All samples show high refractive index that consider as a good candidate in optics and photonics due to their ability to reduce reflection losses [24].

Values of N/m^* and ϵ_∞ were deduced from Figure (12) which represents the dependence of ϵ' on λ^2 . Meanwhile, W_p for free carriers was calculated for both tested samples as a function of laser energies and tabulated in Table (5) with both N/m^* and ϵ_∞ .

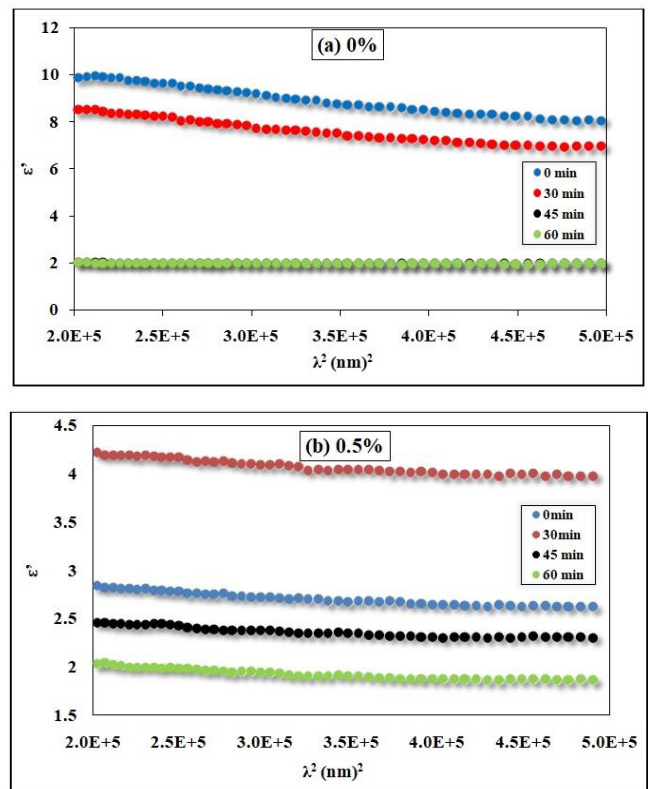


Fig. 12. Variation of optical dielectric constant (ϵ') as a function of $(\lambda)^2$ for a. 0% and b. 0.5% GO loaded PVA/PEG composites

Table (5): Values of optical parameter with respect to both tested samples at different laser beam energies.

Exposure time (min.)	0% GO			0.5% GO		
	ϵ_∞	$(N/m^*)10^{49}$	$(W_p) 10^{11}(\text{Hz})$	ϵ_∞	$(N/m^*)10^{48}$	$(W_p) 10^{10}(\text{Hz})$
0	10	7.7	3	2.8	10	10.1
30	8.5	6.8	2.7	4.3	9.9	10.4
45	2.25	2.2	1.5	2.6	7.7	9.2
60	2.23	1.76	1.3	2.1	2.9	5.6

Table (5) shows that N/m^* values increases with laser dose owing to the increase of free carriers. Moreover, the plasma frequency, W_p , also increases with laser dose.

CONCLUSION

The addition of GO to PVA/PEG (80/20 wt%) leads to a noticeable decrease in optical band gap energy, band tail width, and refractive index. The refractive index dispersion was analyzed on the basis of simple single oscillator model. A decreasing behavior of both E_d and E_s with GO loading is observed due to the increasing behavior in localized electronic state which in turn enhances the low energy transitions. An increasing behavior of W_p with GO loading is

accompanied with the increase of carrier concentration N .

The effect of continuous Argon laser (30 mW) irradiation of samples at different energy doses (exposure time) was assigned. PVA/PEG blend sample loaded with 0.5 wt% GO was selected to study the irradiation effect in comparison with virgin blend due to its considerable absorption behavior.

REFERENCES

- [1] O. Popa, "Preparation and characterization of biopolymer blends based on polyvinyl alcohol and starch," vol. 20, no. 2, pp. 10306–10315, 2015.
- [2] M. Entezam, H. Daneshian, N. Nasirizadeh, H. A. Khonakdar, and S. H. Jafari, "Hybrid Hydrogels Based on Poly(vinyl alcohol) (PVA)/Agar/Poly(ethylene glycol) (PEG) Prepared by High Energy Electron Beam Irradiation: Investigation of Physico-Mechanical and Rheological Properties," *Macromol. Mater. Eng.*, vol. 302, no. 2, pp. 1–9, 2017, doi: 10.1002/mame.201600397.
- [3] A. R. Polu, R. Kumar, and K. V. Kumar, "Ionic conductivity and electrochemical cell studies of new Mg²⁺ ion conducting PVA/PEG based polymer blend electrolytes," *Adv. Mater. Lett.*, vol. 3, no. 5, pp. 406–409, 2012, doi: 10.5185/amlett.2012.6375.
- [4] K. Deshmukh, M. B. Ahamed, and K. K. Sadasivuni, "Graphene oxide reinforced polyvinyl alcohol / polyethylene glycol blend composites as high-performance dielectric material," *J. Polym. Res.*, 2016, doi: 10.1007/s10965-016-1056-8.
- [5] X. Xiao, G. Wu, H. Zhou, K. Qian, and J. Hu, "Preparation and property evaluation of conductive hydrogel using poly (vinyl alcohol)/polyethylene glycol/graphene oxide for human electrocardiogram acquisition," *Polymers (Basel)*, vol. 9, no. 7, pp. 1–15, 2017, doi: 10.3390/polym9070259.
- [6] K. Prabha and H. S. Jayanna, "Influence Of Gamma Irradiation On The Dielectric Properties Of PVA- PS Polymer Blends," vol. 5, no. 8, pp. 5–9, 2015.
- [7] A. M. El Sayed and H. M. Diab, "Controlling the dielectric and optical properties of PVA / PEG polymer blend via e-beam irradiation," 2013, doi: 10.1007/s10965-013-0255-9.
- [8] S. Eve and J. Mohr, "Applied Surface Science Effects of UV-irradiation on the thermo-mechanical properties of optical grade poly (methyl methacrylate)," vol. 256, pp. 2927–2933, 2010, doi: 10.1016/j.apsusc.2009.11.052.
- [9] D. C. Marcano et al., "Marcano2010 Synthesis.Pdf," *Am. Chem. Soc.*, vol. 4, no. 8, 2010.
- [10] R. M. Ahmed, "Optical study on poly(methyl methacrylate)/poly(vinyl acetate) blends," *Int. J. Photoenergy*, vol. 2009, 2009, doi: 10.1155/2009/150389.
- [11] N. F. Mott and E. A. Davis, *Electronic processes in non-crystalline materials*. Oxford university press, 2012.
- [12] D. L. Wood and J. S. Tauc, "Weak absorption tails in amorphous semiconductors," *Phys. Rev. B*, vol. 5, no. 8, p. 3144, 1972.
- [13] C. Wochowski, S. Metev, and G. Sepold, "UV – laser-assisted modification of the optical properties of polymethylmethacrylate," pp. 706–711, 2000.
- [14] M. Fox, *Optical Properties of Solids*, Second Edi. New York: Oxford university press, 2002.
- [15] T. Kardinal and H. Franke, "Photoinduced refractive-index changes in fulgide-doped PMMA films," *Appl. Phys. A Mater. Sci. Process.*, vol. 61, no. 1, pp. 23–27, 1995, doi: 10.1007/s003390050158.
- [16] I. Saini, J. Rozra, N. Chandak, S. Aggarwal, P. K. Sharma, and A. Sharma, "Tailoring of electrical, optical and structural properties of PVA by addition of Ag nanoparticles," *Mater. Chem. Phys.*, vol. 139, no. 2–3, pp. 802–810, May 2013, doi: 10.1016/J.MATCHEMPHYS.2013.02.035.
- [17] S. N. Akhtar et al., "Characterization, electrical and magnetic properties of PVDF films filled with FeCl₃ and MnCl₂ mixed fillers," *Phys. B Condens. Matter*, vol. 406, no. 2, pp. 607–613, 2010, doi: 10.1016/j.physb.2009.10.030.
- [18] S. H. Wemple and M. DiDomenico, "Behavior of the electronic dielectric constant in covalent and ionic materials," *Phys. Rev. B*, vol. 3, no. 4, pp. 1338–1351, 1971, doi: 10.1103/PhysRevB.3.1338.
- [19] M. Kahouli, A. Barhoumi, A. Bouzid, A. Al-Hajry, and S. Guermazi, "Structural and optical properties of ZnO nanoparticles prepared by direct precipitation method," *superlattices Microstruct.*, vol. 85, pp. 7–23, 2015.
- [20] F. Yakuphanoglu, I. S. Yahia, G. Barim, and B. Filiz Senkal, "Double-walled carbon nanotube/polymer nanocomposites: Electrical properties under dc and ac fields," *Synth. Met.*, vol. 160, no. 15–16, pp. 1718–1726, 2010, doi: 10.1016/j.synthmet.2010.06.007.
- [21] A. El-Korashy, H. El-Zahed, and M. Radwan, "Optical studies of [N(CH₃)₄]₂CoCl₄, [N(CH₃)₄]₂MnCl₄ single crystals in the normal paraelectric phase," *Phys. B Condens. Matter*, vol. 334, no. 1–2, pp. 75–81, Jun. 2003, doi: 10.1016/S0921-4526(03)00019-X.
- [22] S. S. Zakariyah et al., "Polymer optical waveguide fabrication using laser ablation," *Proc. Electron. Packag. Technol. Conf. EPTC*, pp. 936–941, 2009, doi: 10.1109/EPTC.2009.5416408.
- [23] L. Ç. Özcan, F. Guay, and L. Martinu, "Investigation of refractive index modifications in CW CO₂ laser written planar optical waveguides," *Opt. Commun.*, vol. 281, no. 14, pp. 3686–3690, Jul. 2008, doi: 10.1016/J.OPTCOM.2008.03.074.
- [24] H. M. Ali, "Characterization of a new transparent-conducting material of ZnO doped ITO thin films," *Phys. Status Solidi Appl. Mater. Sci.*, vol. 202, no. 14, pp. 2742–2752, 2005, doi: 10.1002/pssa.200521045.